Resonant tunneling and negative transconductance in single barrier bilayer graphene structure

V. Hung Nguyen,[1,2,a)] A. Bournel,[1] V. Lien Nguyen,[2] and P. Dollfus[1]
[1]*Institut d'Electronique Fondamentale, UMR8622, CNRS, Universite Paris Sud, 91405 Orsay, France*
[2]*Theoretical Department, Institute of Physics, VAST, P.O. Box 429 Bo Ho, Hanoi 10000, Vietnam*

(Received 9 November 2009; accepted 20 November 2009; published online 11 December 2009)

Using the nonequilibrium Green's function method, the electronic transport in a gate-induced barrier bilayer graphene structure is investigated. Strong resonant effects are shown to result in high amplitude oscillation of conductance as a function of Fermi energy and barrier height. Beyond a small effect of negative differential conductance (with peak to valley ratio less than 2), strong oscillations of transconductance are achieved. The amplitude of such oscillations between positive and negative values may exceed 5 $\mathrm{mS}/\mu\mathrm{m}$. This effect might be helpful for further development of graphene-based nanoelectronics. © *2009 American Institute of Physics*. [doi:10.1063/1.3273376]

Graphene and graphene-based nanostructures have recently attracted a great amount of attention from both experimental and theoretical points of view (see recent reviews).[1,2] Specific properties as the linear dispersion and the chirality of carriers make this material definitely different from conventional solid-state materials.[3] They lead to a number of unusual transport properties such as finite minimal conductivity,[4] unconventional quantum Hall effect,[5] Klein paradox,[3] and so on. In contrast to massless carriers in monolayer graphene (MG), the low energy excitations in bilayer graphene (BG) behave as gapless *massive* chiral Fermions. It leads to the perfect reflection (instead of the perfect transmission in MG) of carriers coming across a barrier with normal incident angle.[3] Additionally, the charge carriers are characterized by Berry's phase 2π in BG while they show a phase π in MG.[5]

Electronic transport in MG structures is fascinating and has been studied systematically, e.g., in Refs. 3–10. However, though the transport properties of some BG structures have been discussed in Refs. 3 and 11, the resonant tunneling effects have not been fully investigated yet. Recently, an efficient calculation method based on the nonequilibrium Green's formalism for solving Dirac's equation has been developed to study the transport properties in graphene-based structures.[9] Using a similar formalism, we investigate here some features associated with resonant tunneling effects and *I-V* characteristics in a gate-controlled barrier BG structure, in particular strong oscillations of transconductance.

BG material consists of two *A-B*-stacked monolayers of graphene. The Hamiltonian, obtained by expanding the momentum close to the ***K***-point[2] in the Brillouin zone, reads

$$H = \begin{pmatrix} \mathrm{v}_F\vec{\sigma}\vec{p} + U & \tau \\ \tau^{\dagger} & \mathrm{v}_F\vec{\sigma}\vec{p} + U \end{pmatrix}, \quad \tau = \begin{pmatrix} 0 & 0 \\ \gamma & 0 \end{pmatrix} \tag{1}$$

with the Pauli matrices $\vec{\sigma} \equiv (\sigma_x, \sigma_y)$, the two-dimensional-momentum vector $\vec{p} \equiv (p_x, p_y)$, the chemical potential U, the Fermi velocity of the monolayer modes $\mathrm{v}_F \approx 10^6$ m/s, and the hopping element between A_2 and B_1 sites $\gamma \approx 0.39$ eV. We study here a typical biased barrier structure as described in Ref. 9, where a finite bias voltage V_b is applied to the electrodes. The potential energy is just considered as a function of x. Though the model is not coupled to Poisson's equation, the barrier of height U_g and width L_g is assumed to be generated and modulated by a gate electrode.[4–6] The assumption, though simple, may highlight fundamental microscopic pictures of charges in graphene-based structures, e.g., the charge conjugation symmetry, the chirality, etc.[3,9]

Similar to that in Ref. 9, the Hamiltonian Eq. (1) is then rewritten in a new basis $\{|x_m\rangle, |k_y\rangle\}$ (with the transverse wave vector $k_y(|k_y\rangle = e^{ik_y y})$ and the mesh spacing $a = x_{m+1} - x_m$) as

$$H_{n,m} = -i\Lambda\delta_{m,n-1} + H_n\delta_{m,n} + i\Lambda\delta_{m,n+1},$$

$$H_n = \begin{pmatrix} U_n + E_y\sigma_y & \tau \\ \tau^{\dagger} & U_n + E_y\sigma_y \end{pmatrix}, \quad \Lambda = E_0\begin{pmatrix} \sigma_x & 0 \\ 0 & \sigma_x \end{pmatrix}, \tag{2}$$

where $E_y = \hbar \mathrm{v}_F k_y$ and $E_0 = \hbar \mathrm{v}_F / 2a$. Using the Hamiltonian Eq. (2), the device Green's function is defined as $G(E) = [E + i0^+ - H_D - \Sigma_L - \Sigma_R]^{-1}$ with the device-contact coupling self-energy $\Sigma_{L(R)}$ calculated from $\Sigma_\alpha = \Lambda g_\alpha \Lambda$. The surface Green's function $g_\alpha = [E + i0^+ - H_\alpha - \Lambda g_\alpha \Lambda]^{-1}$ with the surface Hamiltonian $H_\alpha (\alpha = L, R)$ is solved by using the fast iterative scheme described in Ref. 12. The transmission coefficient needed to calculate the current[8] and the local density of states are defined as: $T(E) = \mathrm{Tr}[\Gamma_L G \Gamma_R G^{\dagger}]$ and $D(x_m, E) = -\mathrm{Im}[G_{m,m}(E)]/\pi$, respectively. The tunneling rate for the left (right) contact is $\Gamma_{L(R)} = i[\Sigma_{L(R)} - \Sigma_{L(R)}^{\dagger}]$. Throughout the work, the mesh spacing a is chosen to be 0.2 nm and unless otherwise stated the temperature is 0 K.

We now investigate transport properties of an unbiased BG structure. The map of local density of states for $E_y = 50$ meV plotted in Fig. 1(a) clearly shows the series of energy gaps and available states in the valence band of the barrier region. Corresponding transmission coefficient T is shown in Fig. 1(b). Note that, differently from MG structures, in the bilayer case Eq. (1) has four possible solutions for a given energy E. Two of them correspond to propagating waves and the other two to evanescent waves.[3] As seen in Fig. 1, the hole bound states (the resonant peaks of T) are very thin and high in comparison with that in the MG barrier.[9] It results from the appearance and strong contribution of evanescent states which make the hole bound states (the resonant peaks of T) narrower with very clear energy

a)Electronic mail: viet-hung.nguyen@u-psud.fr.

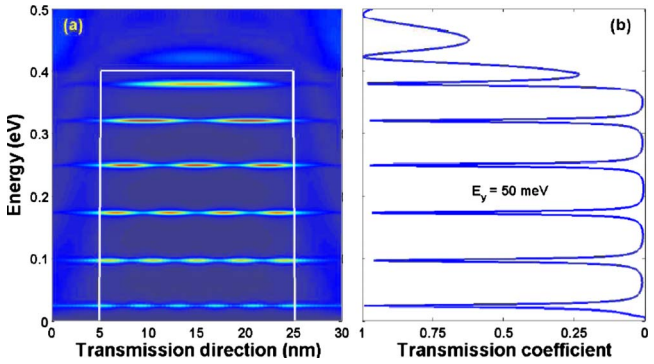

FIG. 1. (Color online) (a) Local density of states for $E_y=50$ meV showing the formation of hole bound states in the barrier region. The white line materializes the barrier profile. (b) Transmission coefficient T as a function of energy E. The structure is unbiased.

gaps between them. Such strong resonant effect is also observed in MG-nanoribbon with finite energy bandgap or using normal conducting contacts.[10] For $E_y=0$ (not shown), there is no bound state in the energy region $E<U_g$, i.e., the normal incident particles are perfectly reflected.[3]

The effects described above of course govern the electrical behavior of the device, e.g., the conductance $\mathcal{G}$ and the current J. In Figs. 2(a) and 2(b), we plot $\mathcal{G}$ as a function of the Fermi energy and the barrier height, respectively. Due to the strong oscillations of T, $\mathcal{G}$ exhibits very high resonant peaks, especially for small L_g. Moreover, by comparing the behavior of $\mathcal{G}$ for different L_g, it is shown that the energy spacing E_s between resonant peaks is proportional to $1/L_g$. Thus, although the dispersion $E \approx \pm \hbar^2 v_F^2 k^2/\gamma$ is parabolic at low energy, the quantization of hole states in the barrier region is still unusual as in MG barrier structures and different from that in conventional materials wherein $E_s \propto 1/L_g^2$.[7,9]

Another interesting feature shown in Figs. 2(a) and 2(b) is the reduction in $\mathcal{G}$-oscillation when increasing L_g. We display in Fig. 2(c) the conductance $\mathcal{G}$ as a function of L_g. It is shown that the amplitude of $\mathcal{G}$ decays exponentially when

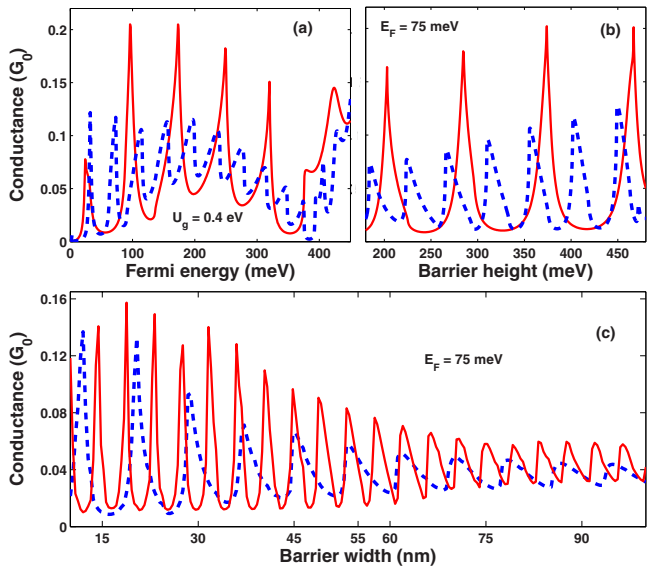

FIG. 2. (Color online) Conductance vs Fermi energy E_F (a) and barrier height U_g (b) for barrier widths $L_g=20$ (solid) and 40 nm (dashed lines). Other parameters are given in the figures. (c) Conductance plotted as a function of L_g for $U_g=0.2$ (dashed) and 0.4 eV (solid line). Everywhere, $E_F=75$ meV. The conductance unit is $G_0=e^2L_y/\pi ha$.

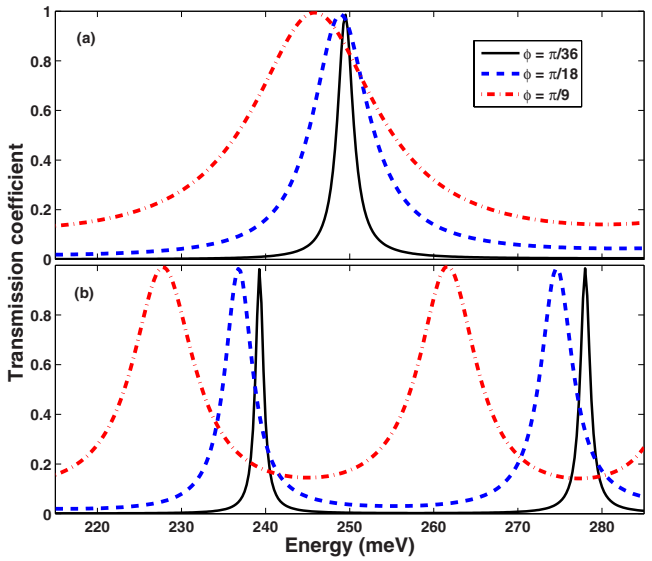

FIG. 3. (Color online) Evolution of transmission coefficient for different incident angles ϕ in two cases: $L_g=20$ (a) and 40 nm (b). Everywhere, $U_g=0.4$ eV.

increasing L_g. Moreover, the decay rate seems to be proportional to $1/U_g$. Thus, the resonant effect is all the stronger that the barrier is thinner and higher. To understand the origin of this behavior, we plot in Fig. 3 the evolution of T for different incident angles $\phi(E_y=\sqrt{E(E+\gamma)}\sin\phi)$ in following two cases: $L_g=20$ (a) and 40 nm (b). For small L_g, the peaks of T are very close to each other. When increasing L_g, their energy spacing is enlarged, which, together with the role of evanescent states, essentially explains the exponential decay of $\mathcal{G}$-oscillation with respect to L_g.

We now explore the I-V characteristics in biased structures. Note that the carriers in graphene are chiral and therefore both electrons and holes (negative energy carriers) can contribute to the current. The current part governed by positive energy carriers can exhibit a significant negative differential conductance (NDC) while the latter one monotonically increases with the bias voltage.[9] This finally results in a quite small NDC in MG-based devices. Due to strong resonant tunneling effects, it is expected that the NDC in BG structure can be stronger than in MG ones. We display in Figs. 4(a) and 4(b) I-V curves for different U_g-values in two cases: $L_g=20$ and 40 nm, respectively. Indeed, the NDC behavior is observed clearly. The peak-to-valley ratio $\kappa=J_p/J_v$, though not so high, can reach the value of $1.7\div2.0$ while it is just about $1.2\div1.3$ in MG structures.[9] However, the most interesting feature observed is not NDC, but the periodical modulation of the current with respect to the barrier height. It originates from the modulation of hole bound states in the barrier region and leads to the oscillation of transconductance $\mathcal{G}_m$ when changing U_g as shown in Fig. 4(c). The current is high when there are some bound states in the energy window $[E_F-eV_b, E_F]$, otherwise, it has a low value. Differently from $\mathcal{G}$, $\mathcal{G}_m$ has both positive and negative values. Its amplitude can reach a significant value of $\sim 5\div8$ mS/μm. This behavior is quite similar to the multiple-valued negative conductance characteristic of the resonant tunneling transistor.[13] Additionally, it is also shown that, on the one hand, the oscillation of $\mathcal{G}_m$ is reduced when increasing L_g [compare Figs. 4(a) and 4(b)], on the other hand, tunning the bias voltage results essentially in a shift of its phase. For

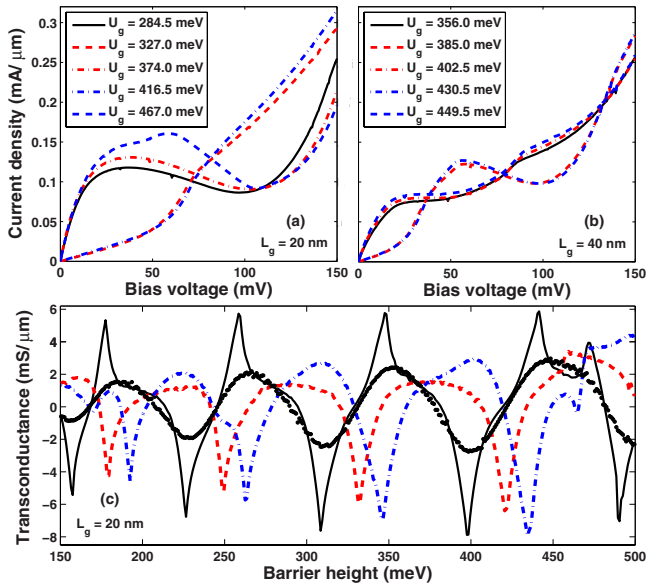

FIG. 4. (Color online) *I-V* characteristics modulated by U_g for L_g=20 (a) and 40 nm (b). Parameters are given in the figures. (c) Transconductance vs U_g for L_g=20 nm in three cases: V_b=40 (solid), 80 (dashed), and 105 mV (dashed-dotted line). The symbols (●) corresponds to the results obtained at the temperature of 77 K and V_b=40 meV. Everywhere, E_F=75 meV.

instance, the phase shift is about π when V_b changes from 40 to 105 mV. It is worth noting that at finite temperature of 77 K, in spite of smearing effects, the oscillations of $\mathcal{G}_m$ are still significant as follows: their amplitude exceeds 2.5 mS/μm [see symbols (●) in Fig. 4(c)]. These electrical behaviors could be used for designing some electronic devices, e.g., high frequency oscillators and multipliers, multistate memories, and logic devices.[13–15]

In summary, by developing a calculation method based on the nonequilibrium Green's function technique, we have investigated the electronic transport through a single barrier BG structure. The structure exhibits very strong resonant effects which manifest in deep valleys and thin peaks of the transmission coefficient and the conductance. Beyond a small effect of NDC, the periodical modulation of *I-V* characteristics by U_g are observed. This leads to strong oscillation of transconductance even at finite temperature. Its amplitude between positive and negative values can exceed 5 mS/μm, Note that, due to the contribution of evanescent states, all relevant quantities related to the *I-V* characteristics reduces exponentially when increasing the barrier width.

This work was partially supported by the European Community through the Network of Excellence NANOSIL and by the French ANR through the project NANOSIM-GRAPHENE.

[1] A. Cresti, N. Nemec, B. Biel, G. Niebler, F. Triozon, G. Cuniberti, and S. Roche, Nano Res. **1**, 361 (2008).
[2] A. H. Castro Neto, F. Guinea, N. M. R. Peres, K. S. Novoselov, and A. K. Geim, Rev. Mod. Phys. **81**, 109 (2009).
[3] M. I. Katsnelson, K. S. Novoselov, and A. K. Geim, Nat. Phys. **2**, 620 (2006).
[4] K. S. Novoselov, A. K. Geim, S. V. Morozov, D. Jiang, M. I. Katsnelson, I. V. Grigorieva, S. V. Dubonos, and A. A. Firsov, Nature (London) **438**, 197 (2005).
[5] K. S. Novoselov, E. McCann, S. V. Morozov, V. I. Fal'ko, M. I. Katsnelson, U. Zeitler, D. Jiang, F. Schedin, and A. K. Geim, Nat. Phys. **2**, 177 (2006).
[6] M. Y. Han, B. Özyilmaz, Y. Zhang, and P. Kim, Phys. Rev. Lett. **98**, 206805 (2007).
[7] J. M. Pereira, Jr., V. Mlinar, F. M. Peeters, and P. Vasilopoulos, Phys. Rev. B **74**, 045424 (2006).
[8] J. M. Pereira, Jr., P. Vasilopoulos, and F. M. Peeters, Appl. Phys. Lett. **90**, 132122 (2007).
[9] V. Nam Do, V. Hung Nguyen, P. Dollfus, and A. Bournel, J. Appl. Phys. **104**, 063708 (2008).
[10] V. Hung Nguyen, V. Nam Do, A. Bournel, V. Lien Nguyen, and P. Dollfus, J. Appl. Phys. **106**, 053710 (2009).
[11] C. Bai and X. Zhang, Phys. Rev. B **76**, 075430 (2007); I. Snyman and C. W. J. Beenakker, *ibid.* **75**, 045322 (2007); J. Nilsson, A. H. Castro Neto, F. Guinea, and N. M. R. Peres, *ibid.* **76**, 165416 (2007).
[12] M. P. Lopez Sancho, J. M. Lopez Sancho, and J. Rubio, J. Phys. F: Met. Phys. **14**, 1205 (1984).
[13] F. Capasso and R. A. Kiehl, J. Appl. Phys. **58**, 1366 (1985).
[14] F. Capasso, S. Sen, F. Beltram, L. M. Lunardi, A. S. Vengurlekar, P. R. Smith, N. J. Shah, R. J. Malik, and A. Y. Cho, IEEE Trans. Electron Devices **36**, 2065 (1989).
[15] N. Yokoyama, K. Imamura, S. Muto, S. Hiyamizu, and H. Nishi, Jpn. J. Appl. Phys., Part 2 **24**, L853 (1985).